

A mechanical model of bacteriophage DNA ejection

Rahul Arun¹

Adlai E. Stevenson High School, 1 Stevenson Drive, Lincolnshire, IL 60069

Sandip Ghosal^{2,*}

*Department of Mechanical Engineering and Engineering Sciences and Applied Mathematics,
Northwestern University, Evanston, IL 60208*

©2017 This manuscript version is made available under the CC-BY-NC-ND 4.0 license
<http://creativecommons.org/licenses/by-nc-nd/4.0/>

DOI: 10.1016/j.physleta.2017.05.044

Abstract

Single molecule experiments on bacteriophages show an exponential scaling for the dependence of mobility on the length of DNA within the capsid. It has been suggested that this could be due to the “capstan mechanism” – the exponential amplification of friction forces that result when a rope is wound around a cylinder as in a ship’s capstan. Here we describe a desktop experiment that illustrates the effect. Though our model phage is a million times larger, it exhibits the same scaling observed in single molecule experiments.

Keywords: bacteriophage, cell mechanics, capstan model, Coulomb-Amontons law, DNA translocation, nanoscale friction

1. Introduction

A bacteriophage is a virus that infects bacterial cells. Like all viruses, they lack the machinery to express the genetic information that they contain. Once

*Corresponding author

Email address: s-ghosal@u.northwestern.edu (Sandip Ghosal)

¹presently at: California Institute of Technology, Pasadena, CA

²phone: (847)467-5990 fax: (847)491-3915 (Sandip Ghosal)

inside their hosts, they “hijack” the cell’s gene transcription mechanism to repli-
 5 cate themselves. Phages are essentially made of two components, a protein
 capsid and the DNA (or RNA in case of RNA phages) that it encloses [1]. In-
 fection is initiated by the phage attaching to the cell membrane followed by
 injection of the DNA into the cell. The capsid remains outside attached to the
 cell membrane.

10 There are several known mechanisms that phages use to inject genetic ma-
 terial into hosts [2, 3, 4, 5]. In most double stranded DNA (dsDNA) phages,
 a fast ejection on the timescale of seconds can be achieved by the release of
 elastic and electrostatic energy of the coiled up DNA confined within the viral
 capsid [6]. This is plausible because dsDNA has a persistence length ~ 50 nm
 15 and a very long strand (e.g. 48.5 kilobase pair or $\sim 17\mu\text{m}$ for the λ phage) is
 packed into a capsid of diameter of the order of the DNA persistence length.
 In fact, for the λ -phage, the internal pressure in the phage capsid is estimated
 to be $\sim 50 - 100$ atmospheres [6]. It is nevertheless unlikely that this mecha-
 nism alone can explain DNA injection in all dsDNA phages. First, the driving
 20 pressure decreases rapidly as DNA empties the capsid; second, the interior of
 bacterial cells have a relatively high osmotic pressure ~ 25 atmospheres that
 would significantly retard DNA entry. In some phages, the DNA ejection takes
 place in two steps. Initially, a part of the DNA is injected by this “coiled spring”
 mechanism. Subsequently, the inserted DNA is expressed to synthesize molecular
 25 motors which then reel in the remainder of the DNA by an ATP driven pulling
 action [7].

In order to understand the ejection process without too many layers of com-
 plexity, *in vitro* experiments have been designed [8] where λ phages are induced
 to eject their DNA into the surrounding buffer in the absence of any host cells.
 30 Here, it is indeed the elastic and electrostatic energy of the tightly coiled DNA
 within the capsid that drives the ejection. Furthermore, in the case of the λ
 phage, the ejection takes place as a single continuous process without pauses and
 stops. The driving force can be calculated from first principles by regarding the
 DNA as a charged semi-flexible rod [9, 10]. The results of such calculations have

35 been confirmed by experiments where the DNA is “stalled” after partial ejection by raising the osmotic pressure in the bath [11, 12]. The speed of ejection, however, is determined not just by the stored potential energy in the capsid but also by the mechanisms of dissipation in the system, and this is more difficult to calculate. Dissipation also plays a role in the opposite process of ATP driven
 40 packaging of DNA into the capsid. In that situation, it determines the time scale for reaching thermodynamic equilibrium. If the packaging rate is fast relative to this time scale then the DNA can take up a more disordered configuration than the ordered one that corresponds to the free energy minimum. On subsequent release from confinement, it encounters a higher frictional resistance as can be
 45 demonstrated in experiments as well as numerical simulations [13, 14].

It has been proposed [15] that the dissipation arises from frictional forces between the DNA and the capsid wall and between neighboring strands as the helically wound DNA slides out of confinement. The frictional interaction is modeled by the classical Coulomb-Amontons laws [16, 17, 18] while disregarding the precise microscopic mechanisms. This is a plausible assumption as the
 50 Coulomb-Amontons laws have been found to hold for nanoscale systems, though the underlying mechanism is quite different from that of the classical picture involving interlocking asperities [19, 20, 21]. The Coulomb-Amontons laws when combined with the equilibrium equations of an elastic rod lead to the conclusion that the tension in the rod increases exponentially with the length of DNA
 55 confined in the capsid [15]. This exponential amplification of tension is a well known fact in mechanics and is known as the “capstan principle”. It is the principle of operation of a winch and various other familiar engineering innovations. The name derives from the cylinder or “capstan” used since antiquity for mooring
 60 ships. Another example of the exponential amplification of friction forces is the extraordinary holding power of phone books with interleaved pages [22, 23]. When applied to the ejection of dsDNA from phages, the capstan principle leads to the conclusion that the ejection velocity per unit driving force (the mobility) should decrease exponentially with the amount of DNA confined within the
 65 capsid at any given instant. This is consistent with *in vitro* experiments on

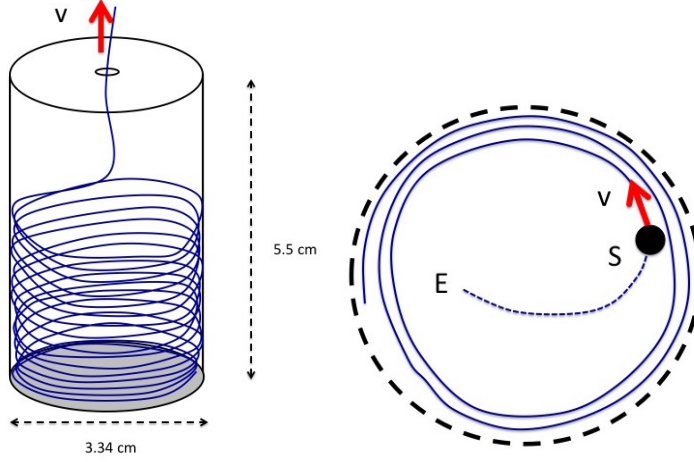


Figure 1: *Left*: Schematic drawing of the mechanical model of a bacteriophage (see Supplementary Materials for photograph and video of experiment). *Right*: Top view showing the spiral arrangement of the nylon fiber within the container. The fluid resistance on the trailing end SE is represented by the drag (kv) on a single hypothetical particle indicated here by the filled circle.

λ -phages [15].

Since the capstan mechanism also operates on macroscopic scales, it should be possible to demonstrate the exponential decrease of mobility on confined length using a centimeter scale model of the phage. In this paper we describe
70 a table top experiment performed using everyday objects that show this dependence. The paper is organized as follows. The main theoretical ideas relating to the capstan effect in phages are summarized in section 2. In section 3 a desktop experiment illustrating the mechanics of DNA ejection from phages is described. In section 4 the data from the experiment is analyzed in the light of the theo-
75 retical ideas discussed earlier in section 2. The significance of the experiment in the context of the DNA-phage problem and its limitations are discussed in section 5. Finally, the main conclusions are summarized in section 6.

2. The Capstan Model

Figure 1 is a schematic diagram of our experimental set up using a plastic
 80 container (representing the viral capsid) and a nylon filament (representing the
 DNA). The question that we wish to answer is the following: how does the
 length of fiber remaining within the capsid (x) vary with time (t) during the
 ejection process?

The driving force F in the ejection process can be obtained from an energy
 85 argument. The driving force due to elasticity of the fiber is the same as the
 inward directed external force F that must be applied to the DNA at the capsid
 exit to prevent it from exiting. The amount of this force can be calculated from
 the principle of virtual work

$$F dx = d\mathcal{F} \quad (1)$$

where $\mathcal{F}(x)$ is the free energy of the DNA. From the theory of linear elasticity,
 90 the elastic bending energy of the DNA may be written as

$$\mathcal{F}(x) = \int_0^x \frac{EI}{2} \kappa^2(s) ds \quad (2)$$

where E is the Young's modulus of the material, I is the area moment of inertia
 of the fiber about the neutral plane, and, $\kappa(s)$ is the local radius of curvature of
 the centerline at a distance ' s ' from the capsid exit. In our mechanical model,
 the volume of nylon fiber inserted is only a small fraction of the capsid volume
 95 so that $\kappa(s) \approx 1/R$, R being the radius of the cylindrical container. Thus, under
 these low packing conditions,

$$\mathcal{F}(x) \approx \frac{EI}{2R^2} x, \quad (3)$$

so that the driving force is

$$F = \mathcal{F}'(x) = \frac{EI}{2R^2}. \quad (4)$$

In the absence of an external stalling force, a tension

$$T(0) = F = \frac{EI}{2R^2} \quad (5)$$

acts on the DNA at the capsid entrance that must be balanced by frictional
100 resistance on the filament arising from within the capsid.

If we assume that the fiber may be described by the equations of elastic equilibrium of a beam and frictional forces are governed by the Coulomb-Amonton law with coefficient of kinetic friction (μ_k), then³ [15]

$$T(s) = T(0) \exp\left(\frac{\mu_k s}{R}\right) = \frac{EI}{2R^2} \exp\left(\frac{\mu_k s}{R}\right), \quad (6)$$

neglecting any reduction in coil radius due to high packing fractions. Equation
105 (6) is the Euler-Eytelwein formula. It is well known for the problem of a flexible or semi-flexible string wrapped around a cylinder [24], but is also applicable, as in this case, to the “inverted” problem of a semi-flexible rod confined within a hollow cylinder [15].

The constant curvature configuration of the beam cannot extend to the extremity E. This is because the internal bending moment is proportional to the
110 curvature and the internal bending moment must vanish at the free boundary E. What this means is that the fiber will lose contact with neighboring strands at some intermediate point S (Figure 1) before E. Determining the true configuration of the fiber under these circumstances then becomes a difficult free
115 boundary problem since neither the location of E nor the shape of the section SE is known apriori. An analogous problem where a beam is pushed onto a hard surface from a point a fixed distance above it has been analyzed recently [25] and is shown to exhibit hysteresis of shape controlled by the static friction coefficient. In Brownian molecular dynamic simulations of bead-chain models,
120 helical arrangements are spontaneously generated except for the trailing ends of the chain [26]. In order to avoid the complexity of having to solve free boundary problems, we introduce a “lumped parameter” model for the resistance (possibly arising out of a combination of frictional and hydrodynamic forces) on the trailing end of the DNA that is not part of the helical arrangement. We do this
125 by supposing that the helically wound fiber is terminated (point S in Figure 1)

³Eq. (13) of [15] contains an error: the factor of 2π in the exponent is superfluous.

by a bead that experiences a hydrodynamic drag kv where $k > 0$ is a drag coefficient. Thus,

$$T(x) = \frac{EI}{2R^2} \exp\left(\frac{\mu_k x}{R}\right) = kv = -k \frac{dx}{dt}. \quad (7)$$

The solution of this differential equation then gives the time dependence of the length x remaining within the capsid

$$x = L - \frac{R}{\mu_k} \ln \left[1 + \frac{EI\mu_k}{2kR^3} \exp\left(\frac{\mu_k L}{R}\right) t \right] \quad (8)$$

130 where L is the length of fiber initially in the capsid ignoring the short section SE. At short times, $t \rightarrow 0$, we have

$$x = L - v_m t \quad (9)$$

where

$$v_m = \frac{EI}{2kR^2} \exp\left(\frac{\mu_k L}{R}\right). \quad (10)$$

Eq. (8) may be rewritten as

$$x = L - \frac{R}{\mu_k} \ln \left(1 + \frac{\mu_k}{R} v_m t \right) \quad (11)$$

and on differentiation,

$$v = -\frac{dx}{dt} = \frac{v_m}{1 + t/\tau} \quad (12)$$

135 where

$$\tau^{-1} = \mu_k v_m / R. \quad (13)$$

Thus, the velocity decreases monotonically from a maximum of v_m on a time scale τ . The total time of ejection T is obtained by setting $t = T$ and $x = 0$ in equation (11)

$$\frac{L}{v_m \tau} = \ln \left(1 + \frac{T}{\tau} \right). \quad (14)$$

Here we have assumed that the length of the residual portion of the fiber that
140 is not ejected may be taken as equal to the length SE in Figure 1.

3. Methods

The bacteriophage model consists of a cylindrical (height, $h=5.5$ cm, radius, $R=1.67$ cm) polyethylene film canister (Fuji 35 mm, type: frosted clear, material: HDPE body, LDPE cap) representing the capsid and a nylon fishing
145 line (Berkley Trilene Big Cat Monofilament Line, 0.55 mm average diameter, 13.6 kg break strength) representing the viral DNA. A centered 2 mm diameter hole was drilled into the top of the film canister through which the monofilament was packaged and ejected. Pieces of filament were pre-cut to the following lengths for the experiment $L_{max} = 50, 100, 150, 200$ and 290 cm. The capsid was
150 loaded by inserting one end of a filament into the container and slowly pushing in a pre-cut section of filament. As soon as the length of filament exceeded some multiple of the canister height, the filament spontaneously arranged itself in a helical pattern against the inside wall of the canister just as observed in Brownian molecular dynamic simulations of DNA-phage systems [26].

155 The filament was confined by covering the exit hole with the thumb and released by removing the thumb. The event was recorded with a movie camera (Drift Innovation HD170 Action Camera, maximum frame rate of 60 fps and resolution 720p) and the ejection time was measured with a stop watch (iPhone 5, Apple Inc.) measuring to 0.01 s. The time between the instant the hole was
160 opened and the instant the filament stopped moving was recorded. In all cases, the ejection stopped with a variable amount of residual length remaining in the capsid. The recorded value of L was taken as the actual length of filament pushed out of the capsid, that is, the true length (L_{max}) minus the residual length. A similar behavior is also seen in the λ phage *in vitro* experiment [8]
165 where there is a long pause between the time when the ejection stops and the time at which the DNA finally separates from the capsid. The experiment was repeated several times with each filament section and the ejected length L and ejection time T was recorded. This data is shown in Section 3, Table 1 of the accompanying Supplementary Material. It is seen that there is a spread in the
170 measured values of L and T by an amount $\Delta L \sim \pm 2$ cm and $\Delta T \sim \pm 0.5$ s.

The experiment was then repeated by submersing the system first in filtered water (Ice Mountain 100 % Natural Spring bottled drinking water) and then in glycerin (Soap Expressions 100 % Vegetable Based). In each case, care was taken to ensure that the liquid completely filled the container without visible air
175 bubbles. The fiber was pre-loaded prior to flooding the container with the fluid. The corresponding ejected length (L) and ejection time (T) data are recorded in Section 3, Table 2 (water) and Table 3 (glycerin) of the accompanying Supplementary Material. The displayed data are an average over four separate runs (three, in the case of the longest fiber length) of the experiment. A still image
180 of the loaded capsid (Section 1) and a slow motion video of the capsid firing (Section 2) are also included.

4. Results

The ejection process appeared qualitatively similar in all three media except for the speed of ejection. In water, the process was slowed down by about a
185 factor of five relative to that in air and by about a factor of almost two hundred in glycerin. Notwithstanding the widely different translocation times, equation (14) provided a good fit to the data in all cases as shown in Figure 2 using the similarity variables $L/(v_m\tau)$ and T/τ . For each data set, the two parameters $v_m\tau$ and τ were chosen to obtain the best fit to equation (14). The fits were
190 arrived at iteratively by trial and error and goodness of fit was decided visually. The best fit parameter values thus obtained are summarized in Table 1. In each of the three cases, the value of the kinetic friction coefficient μ_k inferred from

	Unit	Air	Water	Glycerin
v_m	cm/s	140	70	1.6
τ	s	2.0	1.9	74
μ_k	—	0.006	0.013	0.014

Table 1: Scaling parameters v_m and τ for air, water and glycerin ejections for the data shown in Figure 2. The corresponding friction coefficient μ_k is evaluated from equation (13).

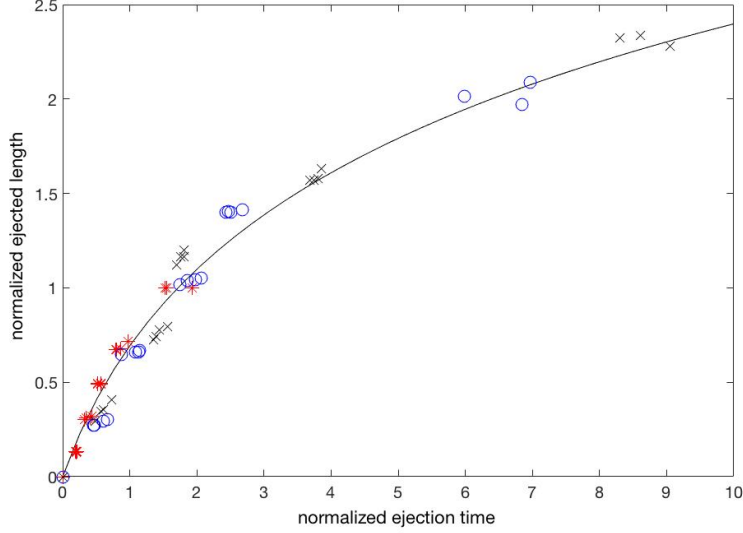


Figure 2: The normalized ejected length $L/(v_m \tau)$ plotted against the normalized ejection time T/τ for air (star), water (circle) and glycerin (cross) ejections. The solid line is equation (14).

equation (13) is also noted. In all three cases, notwithstanding the wide range of velocity and time scales, the friction coefficients are of similar magnitude. Also, the inferred value is not widely different from published values for lubricated polymer materials, though a detailed comparison will not be justified due to the rough nature of these experiments.

5. Discussion

The desktop experiment described here is only meant to illustrate the part of the DNA-phage system behavior relating to the capstan mechanism and is not necessarily an appropriate model for all aspects of the DNA ejection problem in phages. Indeed the two systems differ widely in spatial scales as well as in the details of the physical interactions that control their behavior.

An important difference between the current experiment and the real DNA-phage system is the extent of packing of the capsids. In λ -phage, the volume of the polymer relative to the maximum available capsid volume (the packing

fraction, f) is in the range $0.4 - 0.5$ [27]. In the mechanical model presented here, the packing fraction is easily estimated from the geometric parameters in section 3, $f \approx 0.002 - 0.015$, much smaller than the actual values encountered in
210 phages. The behavior at high packing fractions has been explored recently using macroscopic mechanical models to represent the phage-DNA system [28, 29, 30]. The focus of these investigations is the shape acquired by the packed DNA inside the capsid rather than the dynamics of ejection studied here. Also, the metal wires used have significantly higher plasticity than the nylon fibers used in the
215 present experiments.

The low packing fractions used here is also responsible for an important qualitative difference between our model and the real phage system. Measured ejection velocities in the λ phage when plotted as a function of the DNA remaining within the capsid show a characteristic unimodal shape. That is, the
220 escape velocity first increase as the capsid starts to empty, reaches a maximum at an intermediate stage and finally decreases. This is because the velocity $v = F(x)m(x)$ where the mobility $m(x) \propto \exp(-bx)$ ($b > 0$) but the driving force F is an increasing function of x since the capsid pressure increases as the capsid is tightly packed. In fact, when the steric constraint is accounted for,
225 $F(x) \propto (1 - x/x_m)^{-1}$ where x_m is the maximum length of DNA that the capsid can accommodate [9, 10]. In the experiment described here, the volume fraction of fiber inserted was small compared to the maximum capacity of the capsid, to avoid jamming and other practical complications. Thus, $F(x)$ is a constant given by equation (4) so that the velocity decreases monotonically rather than
230 show a peak at an intermediate time.

The scale of the DNA-phage problem is such that any hydrodynamic interactions would be firmly in the Stokesian regime, that is, the Reynold's number $Re = \rho v d / \mu$, where ρ is the fluid density, μ is the viscosity, v is a characteristic velocity and d is a characteristic length, is essentially zero. In our mechanical
235 model, using the exit hole diameter (2 mm) as a length scale and the maximum value of the ejection velocity v_m as the velocity scale, we find $Re = 374$, 1 and 0.02 respectively for ejections in air, water and glycerin. Thus, only

the glycerin experiments truly represent the hydrodynamic conditions in the DNA-phage system. However, we find that the scaling law, equation (14), holds
 240 irrespective of the working fluid though the ejection velocity itself depends on fluid viscosity. This is consistent with the capstan model that attributes the exponential dependence of mobility on filament length to interstrand friction, and fluid viscosity only plays an incidental role [15].

The pressure within the viral capsid ejecting the DNA arises from a combination of the bending energy of the DNA and the electrostatic self-repulsion
 245 between strands. These two factors contribute about equally to the potential energy of the confined DNA [6]. The electrostatic part of the potential energy can be readily tuned by changing the ionic composition of the solvent and thereby changing the Debye length. At high ionic concentrations and in the presence of polyvalent ions such as Mg^{2+} the DNA backbone charge is almost
 250 perfectly shielded, reducing the electrostatic self-repulsion to almost zero. Ionic composition changes are found to affect the ejection speed in experiments [8] mainly through its effect on the capsid pressure. Numerical simulations suggest [31] that the topology of the DNA configuration during the packaging phase can depend on the ionic composition of the bath. When the packaged DNA is
 255 allowed to eject freely, the ejection speed could in turn depend on the topology of the packaged strand [32]. These aspects of the problem of course cannot be accessed using our mechanical model as the stored potential energy in our nylon fiber is purely elastic; unlike DNA, it does not have an electrostatic component.

260 6. Conclusion

Recent advances in single molecule observation and manipulation have made it possible to study the packaging [33] and ejection [8] of DNA from phages with *in vitro* techniques. Such experiments have resulted in quantitative data that require explanations and interpretations. These problems belong to the
 265 “mesoscale” where the familiar classical mechanics of solids and fluids may still be applied but often in association with effects such as statistical fluctuations

and Debye layer physics that are peculiar to small scale systems. In this paper, we consider one such problem, bridging a gap of almost seven orders of magnitude to take ideas very familiar in marine engineering (winches and capstans) and applying them in the realm of cell biology (phages and DNA).

The specific single molecule experiment of interest here involves the ejection of DNA by the λ phage into the surrounding buffer. It was shown that the experimental data on ejection velocity is consistent with a frictional resistance law that has an exponential dependence on the length of DNA in the capsid. A possible mechanism for this was suggested [15] based on the “capstan effect”, where the helical geometry of the DNA together with the Coulomb-Amonton friction law results in an exponential amplification of friction with increasing turns.

The conditions required for the capstan mechanism can be simulated in a large scale system just as easily as in the bacteriophage. In this paper we have presented results from a desktop experiment that mimicks the process of DNA ejection from bacteriophages. The measured ejection time as a function of ejected length was found to be consistent with a scaling law derived on the basis of the capstan model. The scaling law was found to be independent of the Reynold’s numbers in the range $\sim 0.01 - 300$.

This research did not receive any specific grant from funding agencies in the public, commercial, or not-for-profit sectors.

Acknowledgement

We wish to thank Prof. Sigurdur Thoroddsen (King Abdullah University of Science and Technology) for helpful suggestions and the Department of Mechanical Engineering, Northwestern University for loan of the video camera.

References

References

- [1] C. M. Knobler and W. M. Gelbart. Physical Chemistry of DNA Viruses, *Annual Review of Physical Chemistry*, 60(1):367–83, May 2009.
- [2] I. J. Molineux. Fifty-three years since Hershey and Chase; much ado about pressure but which pressure is it? *Virology*, 344(1):221–229, January 2006.
- [3] M. M. Inamdar, W. M. Gelbart, and R. Phillips. Dynamics of DNA Ejection from Bacteriophage. *Biophysical Journal*, 91(2):411–420, July 2006.
- [4] P. Grayson and I. J. Molineux. Is phage DNA ‘injected’ into cells - biologists and physicists can agree. *Current Opinion in Microbiology*, 10(4):401–409, August 2007.
- [5] I. J. Molineux and D. Panja. Popping the cork: mechanisms of phage genome ejection. *Nature Reviews Microbiology*, 11(3):194–204, March 2013.
- [6] M. De Frutos, A. Leforestier, and F. Livolant. Relationship between the genome packing in the bacteriophage capsid and the kinetics of dna ejection. *Biophysical Reviews and Letters*, 09(01):81–104, November 2013.
- [7] V. González-Huici, M. Salas, and J. M. Hermoso. The push–pull mechanism of bacteriophage ϕ 29 DNA injection. *Molecular Microbiology*, 52(2):529–540, March 2004.
- [8] P. Grayson, L. Han, T. Winther, and R. Phillips. Real-time observations of single bacteriophage λ DNA ejections in vitro. *Proceedings of the National Academy of Sciences of the United States of America*, 104(37):14652–14657, September 2007.
- [9] P. K. Purohit, J. Kondev, and R. Phillips. Mechanics of DNA Packaging in Viruses. *Proceedings of the National Academy of Sciences*, 100(6):3173–3178, March 2003.

- [10] P. K. Purohit, M. M. Inamdar, P. D. Grayson, T. M. Squires, J. Kondev, and R. Phillips. Forces during Bacteriophage DNA Packaging and Ejection. *Biophysical Journal*, 88(2):851–866, February 2005.
- [11] A. Evilevitch, L. Lavelle, C. M. Knobler, E. Raspaud, and W. M. Gelbart. Osmotic pressure inhibition of DNA ejection from phage. *Proceedings of the National Academy of Sciences*, 100(16):9292–9295, August 2003.
- [12] A. Evilevitch, M. Castelnovo, C. M. Knobler, and W. M. Gelbart. Measuring the Force Ejecting DNA from Phage. *J. Phys. Chem. B*, 108(21):6838–6843, 2004.
- [13] Z. T. Berendsen, N. Keller, S. Grimes, P. J. Jardine, and D. E. Smith. Nonequilibrium dynamics and ultraslow relaxation of confined DNA during viral packaging. *Proceedings of the National Academy of Sciences*, 111(23):8345–8350, June 2014.
- [14] L. R. Comolli, A. J. Spakowitz, C. E. Siegerist, P. J. Jardine, S. Grimes, D. L. Anderson, C. Bustamante, and K. H. Downing. Three-dimensional architecture of the bacteriophage ϕ 29 packaged genome and elucidation of its packaging process. *Virology*, 371(2):267–277, February 2008.
- [15] S. Ghosal. Capstan Friction Model for DNA Ejection from Bacteriophages. *Physical Review Letters*, 109(24):248105, December 2012.
- [16] C. Marone. Laboratory-Derived Friction Laws and Their Application to Seismic Faulting. *Annual Review of Earth and Planetary Sciences*, 26(1):643–696, 1998.
- [17] B. N. J. Persson. *Sliding Friction: Physical Principles and Applications*. Springer, July 2000.
- [18] F. P. Bowden and D. Tabor. *The Friction and Lubrication of Solids*. Oxford University Press, April 2001.

- [19] Y. Mo, K. T. Turner, and I. Szlufarska. Friction laws at the nanoscale. *Nature*, 457(7233):1116–1119, February 2009.
- [20] J. Gao, W. D. Luedtke, D. Gourdon, M. Ruths, J. N. Israelachvili, and U. Landman. Frictional Forces and Amontons’ Law: From the Molecular to the Macroscopic Scale. *The Journal of Physical Chemistry B*, 108(11):3410–3425, March 2004.
- [21] E. Gnecco, R. Bennewitz, T. Gyalog, C. Loppacher, M. Bammerlin, E. Meyer, and H.-J. Güntherodt. Velocity Dependence of Atomic Friction. *Physical Review Letters*, 84(6):1172–1175, February 2000.
- [22] H. Alarcón, T. Salez, C. Poulard, J.-F. Bloch, É. Raphaël, K. Dalnoki-Veress, and F. Restagno. Self-Amplification of Solid Friction in Interleaved Assemblies. *Physical Review Letters*, 116(1):015502, January 2016.
- [23] K. Dalnoki-Veress, T. Salez, and F. Restagno. Why can’t you separate interleaved books? *Physics Today*, 69(6):74–75, May 2016.
- [24] I. M. Stuart. Capstan equation for strings with rigidity. *British Journal of Applied Physics*, 12(10):559–562, October 1961.
- [25] T. G. Sano, T. Yamaguchi, and H. Wada. Slip Morphology of Elastic Strips on Frictional Rigid Substrates. *Physical Review Letters*, (118):178001, April 2017.
- [26] J. Kindt, S. Tzlil, A. Ben-Shaul, and W. M. Gelbart. DNA Packaging and Ejection Forces in Bacteriophage. *Proceedings of the National Academy of Sciences*, 98(24):13671–13674, November 2001.
- [27] P. Grayson, A. Evilevitch, M. M. Inamdar, P. K. Purohit, W. M. Gelbart, C. M. Knobler, and R. Phillips. The effect of genome length on ejection forces in bacteriophage lambda. *Virology*, 348(2):430–436, May 2006.
- [28] M. A. F. Gomes, V. P. Brito, and M. S. Araújo. Geometric properties of crumpled wires and the condensed non-solid packing state of very long

molecular chains. *Journal of the Brazilian Chemical Society*, 19(2):293–298, 2008.

- [29] T. A. Sobral, M. A. F. Gomes, N. R. Machado, and V. P. Brito. Un-
packing of a Crumpled Wire from Two-Dimensional Cavities. *PLOS ONE*,
375 10(6):e0128568, June 2015.
- [30] V. H. de Holanda and M. A. F. Gomes. Scaling, crumpled wires, and
genome packing in virions. *Physical Review E*, 94(6):062406, December
2016.
- [31] I. Ali and D. Marenduzzo. Influence of ions on genome packaging and
380 ejection: a molecular dynamics study. *The Journal of Chemical Physics*,
135(9):095101–095101, September 2011.
- [32] D. Marenduzzo, C. Micheletti, E. Orlandini, and D. W. Sumners. Topolog-
ical friction strongly affects viral DNA ejection. *Proceedings of the National
Academy of Sciences*, 110(50):20081–20086, December 2013.
- [33] D. E. Smith, S. J. Tans, S. B. Smith, S. Grimes, D. L. Anderson, and
385 C. Bustamante. The bacteriophage ϕ 29 portal motor can package DNA
against a large internal force. *Nature*, 413(6857):748–752, October 2001.

List of supplementary material

The following supplementary material accompanies this paper

- 390 1. Photograph illustrating experimental set up.
2. Video of experiment in progress.
3. Tabular data of measured ejection times.

Supplementary Material*

“A mechanical model of bacteriophage DNA ejection”

Rahul Arun & Sandip Ghosal

1 Photograph illustrating experimental set up



Figure 1: Photograph of mechanical model. *Capsid* – 35 mm Fuji film canister (Type: frosted clear, Body: HDPE, Cap: LDPE). *DNA* – Nylon Monofilament fishing line, brand: Berkley Trilene Big Cat 0.022 in (0.55mm) average diameter, break strength 30 lb (13.6 kg).

*©2017 This manuscript version is made available under the CC-BY-NC-ND 4.0 license <http://creativecommons.org/licenses/by-nc-nd/4.0/> DOI: 10.1016/j.physleta.2017.05.044

2 Video of experiment in progress

Video file: VideoAirSlowMo1.mov
(available from corresponding author upon request)

Video Descriptor:

Video of nylon monofilament with 5 cm color bands (for enhanced visibility) ejected from the film canister representing the viral capsid. The medium in this case is air. The “Drift Innovation HD170” Action Camera was used with a Frame Rate of 60 FPS and a resolution of 720p. The video is slowed down by a factor of 8.

3 Tabular data of measured ejection times

The data points shown in Figure 2 of the paper are as follows:

Length (cm)	Time (s)
0.0	0.00
36.0	0.40
37.0	0.38
37.0	0.41
37.0	0.43
85.0	0.66
87.0	0.71
87.0	0.81
90.0	0.86
137.0	1.05
137.0	1.13
139.0	1.03
139.0	1.13
188.0	1.60
189.0	1.58
190.0	1.73
200.0	1.96
279.6	3.05
279.6	3.85
280.3	3.10

Table 1: Ejected length vs time for ejections in air

Length (cm)	Time (s)
0.0	0.00
36.0	0.88
36.0	0.90
39.0	1.15
40.0	1.26
86.0	1.66
88.0	2.05
88.0	2.15
89.0	2.18
135.0	3.32
138.0	3.53
139.0	3.75
140.0	3.93
186.0	4.63
186.0	4.76
187.0	4.70
188.0	5.08
261.9	13.01
267.8	11.38
278.0	13.23

Table 2: Ejected length vs time for ejections in water

Length (cm)	Time (s)
0.0	0.00
35.0	35.91
41.0	42.40
42.0	44.60
48.0	54.40
86.0	100.10
88.0	103.35
92.0	106.63
94.0	115.51
133.0	125.16
138.0	130.16
138.0	133.65
142.0	133.99
186.0	272.18
186.0	276.76
187.0	281.21
193.0	284.87
270.1	670.00
275.1	614.00
276.8	637.00

Table 3: Ejected length vs time for ejections in glycerin